Получение, структура, свойства

UDC 549/548.211

Surface morphology and structural types of natural impact apographitic diamonds

V. Kvasnytsya[1,*], R. Wirth[2], S. Piazolo[3], D. E. Jacob[3], P. Trimby[4]

[1]Institute of Geochemistry, Mineralogy and Ore Formation, National Academy of Sciences of Ukraine, Kyiv, Ukraine

[2]Helmholtz-Centre Potsdam, German Research Centre for Geosciences, Potsdam, Germany

[3]Australian Research Council Centre of Excellence for Core to Crust Fluid Systems and Department of Earth and Planetary Sciences, Macquarie University, North Ryde, Australia

[4]Australian Centre for Microscopy and Microanalysis, The University of Sydney, Australia

**vmkvas@hotmail.com*

External and internal morphologies of natural impact apographitic diamonds (paramorphoses) have been studied. The (0001) surface morphology of the paramorphoses reflects their phase composition and the structural relationship of their constituting phases. Growth and etch figures together with the elements of crystal symmetry of lonsdaleite and diamond are developed on these surfaces. The crystal size of lonsdaleite is up to 100 nm, and that of diamond is up to 300 nm. Two types of structural relations between graphite, lonsdaleite, and diamond in the paramorphoses are observed: the first type (black, black-gray, colorless and yellowish paramorphoses) – (0001) graphite is parallel to $(10\bar{1}0)$ *lonsdaleite and parallel to (111) diamond; the second type (milky-white paramorphoses) – (0001) graphite is parallel to* $(10\bar{1}0)$ *lonsdaleite and parallel to (112) diamond. The first type of the paramorphoses contains lonsdaleite–diamond–graphite or diamond–lonsdaleite, the second type of the paramorphoses contains predominantly diamond. The direct phase transition of graphite → lonsdaleite and/or graphite → diamond occurred in the paramorphoses of the first type. A successive phase transition graphite → lonsdaleite → diamond was observed in the paramorphoses of the second type. The structure of the paramorphoses of this type shows characteristic features of recrystallization.*

Keywords*: natural impact apographitic diamond, graphite, lonsdaleite, diamond, surface morphology, structure type.*

INTRODUCTION

Impact diamonds are observed in many meteorite craters of the Earth [1–4]. In most of the known craters these diamonds are paramorphoses on graphite crystals mimicking their primary form with some deviation from their original hexagonal contours [1–4]. There are a few basic varieties of the paramorphoses based on color and transparency: opaque black, opaque gray–black, opaque milky–white, colorless, and transparent yellowish. Despite the external appearance of single graphite crystals, the paramorphoses have a multiphase composition. They are textured polycrystalline and polyphase formations consisting of strictly oriented micro-nanocrystallites of the new phases such as lonsdaleite and diamond and some relict or newly formed graphite [1, 2]. The ratios of these three phases in the paramorphoses can be different. X-ray diffraction study of powder samples of the paramorphoses showed different ratios of crystalline phases for the paramorphoses of different colors [1]. Black paramorphoses can contain up to 37 % or more lonsdaleite (the rest is composed of graphite and diamond), colorless and yellowish paramorphoses contain up to 20–25 % lonsdaleite (the rest is diamond), and milky–white paramorphoses contain only a small fraction of lonsdaleite; they are almost pure diamond. This is the highest content of lonsdaleite observed in the three-phase paramorphoses.

X-ray studies of natural impact apographitic diamonds, theoretical developments and comparison with the products of experimental shock transformation of graphite revealed a martensitic mechanism of their formation [5]. It was suggested that the direct coherent transitions of graphite to lonsdaleite and graphite to diamond occurred during natural shock compression, experimental shock and static compression [1, 6]. The successive transformation of graphite → lonsdaleite → diamond was established for experimental shock-quenched diamond [6]. Generally, the new crystalline phases (lonsdaleite, diamond) are strictly oriented to each other and relative to the original graphite crystal. Consequently, the growth and etch figures on the (0001) surfaces of paramorphoses should reflect the relative orientation of both phases and their own symmetry.

In principle, the crystallographic characteristics including symmetry relationships and anisotropic surface reactivity, and surface energy are expected to result in distinct growth and etch figures dependent on the crystallographic orientation of the surface, e.g., [7, 8]. For example, it has been demonstrated that the growth and etch figures on the (0001) surfaces of the paramorphoses allow us to qualitatively assess the phase composition and to establish the orientation relationship between the original and newly formed phases [9]. This data allows the establishing of a mechanism of the active phase transitions. The present study is a continuation of the aforementioned micromorphology study of the paramorphoses of different color and an identification of the mechanism of their formation. Our paper reports the first observation of new structural type of natural impact apographitic diamond. The major aim of this paper is to present morphological and textural data and observations of this unusual impact diamond, as obtained by modern techniques. This diamond is interpreted as product of growth at very high temperatures and pressures.

SAMPLES AND ANALYTICAL TECHNIQUES

Many small impact apographitic diamonds – paramorphoses – from Popigai meteor crater (Russia) have been investigated (Fig. 1). The crystal size varies from approximately 0.10 to 0.75 mm. On the (0001), $(10\bar{1}0)$ surfaces as well as on fracture surfaces of these paramorphoses twin striation, growth and etch figures are

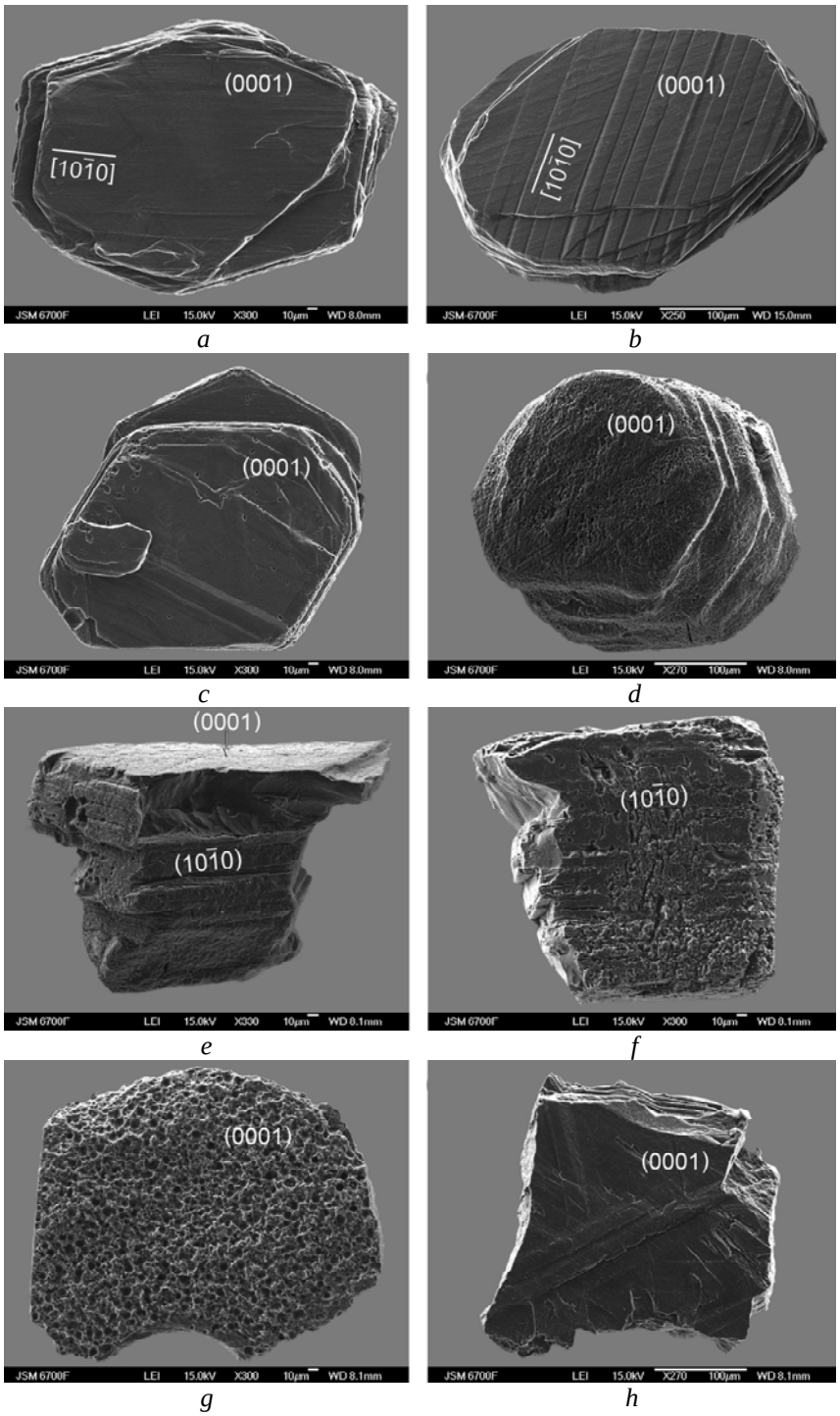

Fig. 1. SEM images of different natural impact apographitic diamonds (a–f are rare paramorphoses; g, h are common paramorphoses): *a* – on the (0001) face of the paramorphose there is a thin twin striation visible along [10$\bar{1}$0]; *b* – on the (0001) face of the paramorphose there is an intense twin striation visible along [10$\bar{1}$0]; *c* – a paramorphose formed on original twin graphite crystals after Veselovsky's law; *d* – a paramorphose formed on parallel intergrowths of original graphite crystals; *e*, *f* – the paramorphoses formed on pinakoid-prismatic original graphite crystals; *g* – a paramorphose with intense etching of the (0001) surface; *h* – fragment of a paramorphose, which is a common form of the impact apographitic diamonds.

observed. A scanning electron microscopy (SEM) was used to study of the morphology of these surfaces. For phase composition study of the paramorphoses transmission electron microscopy (TEM) was used. SEM investigations were carried out on a JSM-6700F (JEOL) equipped with an energy dispersive X-ray analyzer at Semenenko Institute of Geochemistry, Mineralogy and Ore Formation of National Academy of Sciences, Kyiv, Ukraine.

Two paramorphoses of different colors were selected for TEM study: 1 is black and opaque; 2 is milky-white and opaque. Electron transparent foils for TEM investigation were prepared in a focused ion beam (FIB) device (FIB 200 TEM) at GFZ Potsdam, Germany. The foils were cut approximately parallel to $(10\bar{1}0)$ planes of the paramorphoses. Details about FIB sample preparation are given elsewhere [10, 11]. TEM investigations were performed on a FEI Tecnai F20 XTwin with a field emission gun as electron emitter. The TEM is equipped with an EDAX X-ray analyzer, a Gatan imaging filter GIF Tridiem and a high-angle annular dark field detector. TEM techniques such as electron diffraction and high-resolution lattice fringe imaging were applied to the samples.

In order to determine the orientation relationships at a μm to nm scale, two representative FIB foils of the TEM studied paramorphoses were measured using Transmission Kikuchi Diffraction (TKD analysis). This new technique allows orientation and phase recognition at the nm scale in sample where conventional Electron Backscatter Diffraction is at its limits [12]. This analysis was performed using a Zeiss Ultra Plus FEG SEM, equipped with an Oxford Instruments Channel 5 EBSD system and a Nordlys-S EBSD detector at Australian Centre for Microscopy and Microanalysis, the University of Sydney operated at 1–10 nA and 30 kV at high vacuum. The TEM foil was mounted using custom made clamps attached to a standard 70° tilted EBSD sample holder. The SEM stage was tilted toward the EBSD detector by 20 degrees at a working distance of typically 5 mm from the pole piece [12]. After positioning of the SEM stage the EBSD detector including phosphorous screen and fore scatter detectors was fully inserted. Orientation maps were collected by stepping the electron beam across the surface in a rectangular grid with a step size of 10 nm. Diffraction patterns were collected with a resolution of 336×256 pixel (4×4 binning). During data acquisition all patterns were stored and later re-analyzed with optimal conditions for the band detection. The orientation and intensity of 11 Kikuchi band were compared to up to 49 theoretical bands [13] to calculate the orientation of each analysis point. EBSD data are presented in the form of (i) relative orientation maps exhibiting changes in crystallographic orientation relative to a chosen reference orientation, (ii) lower hemisphere pole figures where X and Y directions correspond to the horizontal and vertical sample reference frame and (iii) orientation contrast images.

RESULTS

SEM investigations

Depending on the phase composition, to be more specific the ratio between lonsdaleite and diamond, the surfaces of the paramorphoses display various growth and etch figures. At the most advanced (0001) surface of the paramorphoses the symmetry of these figures corresponds to the symmetry of planes of lonsdaleite or diamond. On the $(10\bar{1}0)$ surface of the paramorphoses this dependence is almost manifested through a thin layer of (0001) graphite. However on all surfaces of the paramorphoses, including fracture surfaces, twin striations along $(11\bar{2}1)$ are visible

(Fig. 2, *a*). The intensity of the twin striation development is different from grain to grain and it depends to some extent on the phase composition of the paramorphoses.

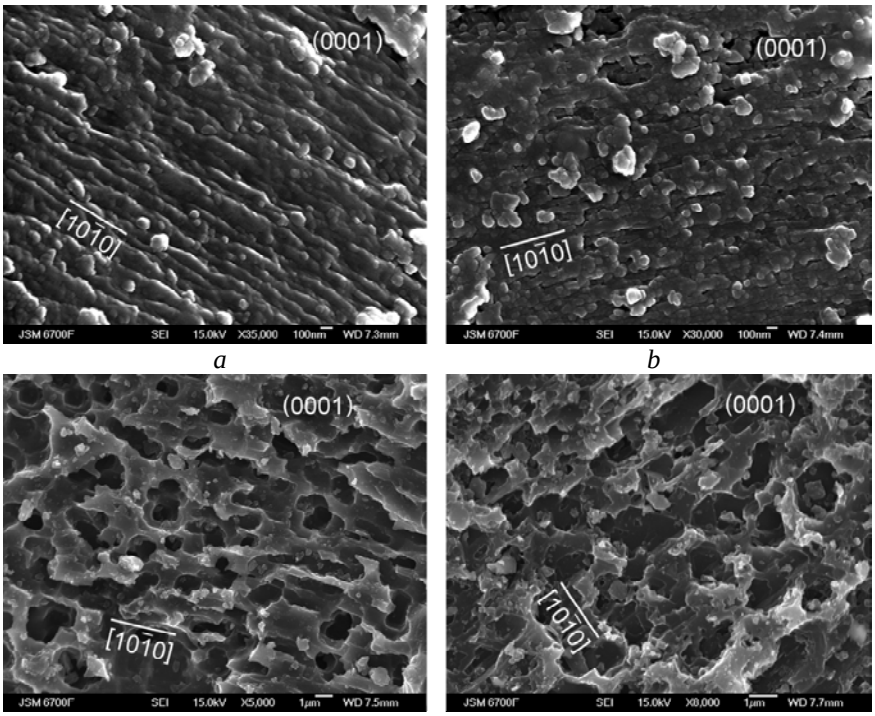

Fig. 2. SEM images of new figures on the (0001) surfaces of natural impact apographitic diamonds (*a*–*c* are black paramorphoses, *d* is a yellowish paramorphose): *a* – the traces of intense twinning; *b* – rectangular growth plates; *c* – rectangular etch pits; *d* – trigonal and hexagonal etch pits. All new figures are strictly oriented along [10$\bar{1}$0].

The black paramorphoses contain three phases, often with dominance of lonsdaleite. Typically, the (0001) surfaces of such paramorphoses are covered with rectangular figures of growth and etching (see Fig. 2, *b*, *c*). These figures are oriented along the [10$\bar{1}$0] direction. The size of rectangular growth planes is up to 100 nm.

The colorless and slightly yellowish paramorphoses contain less lonsdaleite and more diamond. On their (0001) surfaces trigonal and hexagonal etch pits are often visible (see Fig. 2, *d*). The patterns of such cavities are oriented along the [10$\bar{1}$0] direction. They testify the prevailing diamond phase in the paramorphoses. The same cavities cover the faces of the octahedron of natural diamonds.

The milky-white paramorphoses are unique. They consist almost of pure diamond. The external hexagonal form of these paramorphoses is very rare. However, twin striation along [10$\bar{1}$0] direction occurs sometimes on such paramorphoses. Most of these paramorphoses were created by etching. Numerous negative rectangular and quadratic pyramidal pits cover the (0001) surfaces (Fig. 3). The same cavities cover the faces of the trapezohedrons and cube of natural diamonds, respectively. However, depending on the inclination of the surface (0001) the walls of these pits and pyramids display trigonal or hexagonal or quadratic or rectangular symmetry (Fig. 4). All of these etch figures are strictly oriented along [10$\bar{1}$0].

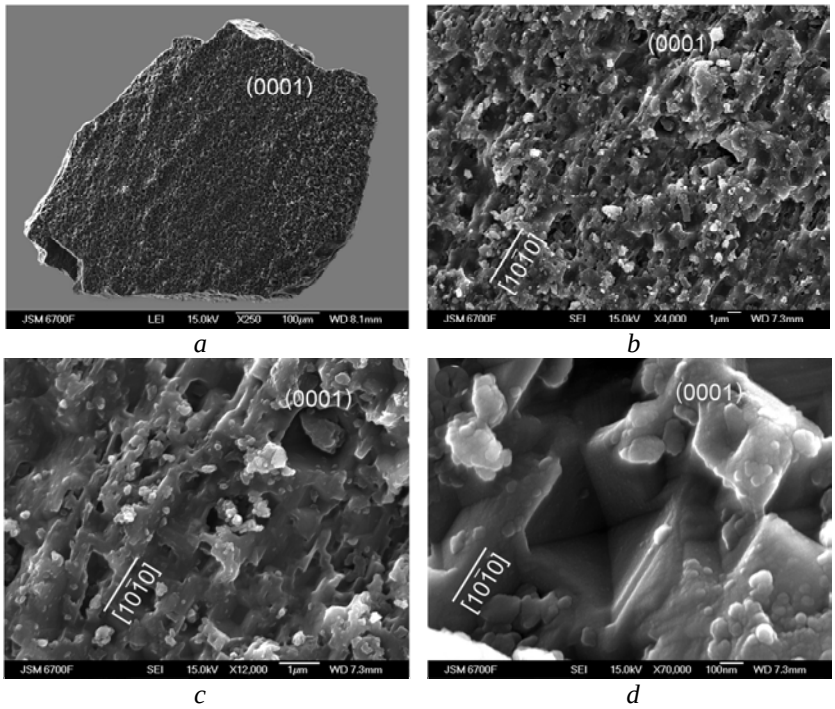

a *b* *c* *d*

Fig. 3. SEM images of natural impact apographitic diamond and its new etch figures on the (0001) surface: *a* – morphology of milky-white paramorphose; *b* – (0001) surface covered by rectangular and quadratic pyramidal etch pits oriented along [10$\bar{1}$0]; *c*, *d* – details of the etch pits.

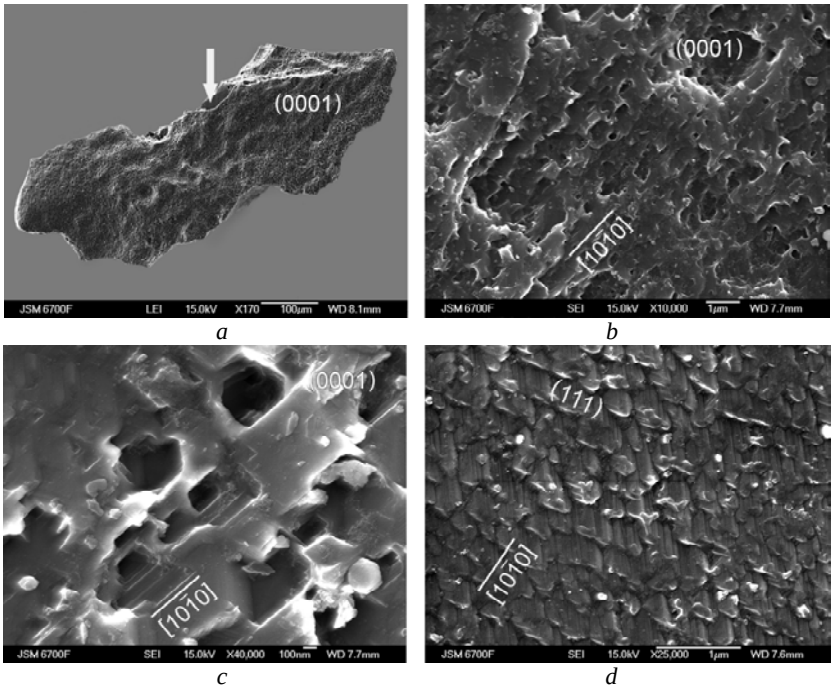

a *b* *c* *d*

Fig. 4. SEM images of natural impact apographitic diamond and its new figures on the (0001) surface and on the breaking surface: *a* – morphology of a milky-white paramorphose; *b* – (0001) surface of the paramorphose covered by rectangular and quadratic pyramidal etch pits oriented along [10$\bar{1}$0]; *c* – details of the etch pits; *d* – the patterns of diamond octahedrons on the breaking surface. The breaking surface is indicated by the white arrow (*a*).

On fracture surfaces of milky-white paramorphoses the patterns of octahedral diamond crystallites (see Fig. 4) are observed, which are strictly oriented along the $[10\bar{1}0]$ direction. Their size does not exceed 300 nm. A notable feature of milky-white paramorphoses is the epitaxial growth of diamond on the (0001) surfaces. The tiny diamond octahedrons grow on the diamond matrix of these paramorphoses (Fig. 5). Their size does not exceed 2–10 μm.

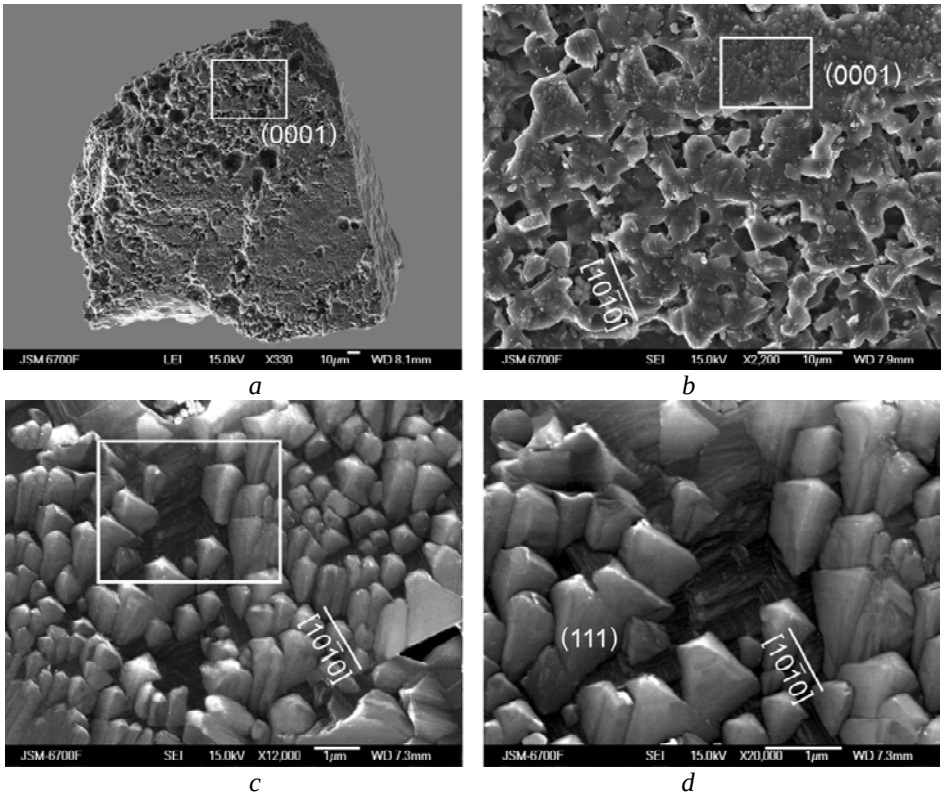

a *b* *c* *d*

Fig. 5. SEM images of natural impact apographitic diamond with oriented micro-nanopolyhedrons of diamonds – octahedrons grown on its (0001) surface, often L_4 axis of octahedrons is parallel to [001] diamond matrix: *a* – morphology of a milky-white paramorphose; *b* – (0001) surface of the paramorphose covered by diamond octahedrons; *c*–*d* – details of octahedrons (their locations in the images *a*, *b*, and *c* is indicated by white rectangle).

TEM investigations

For these investigations we have chosen two extreme types of impact diamonds: with domination of lonsdaleite and diamond. Figures 6 and 7 show the paramorphoses studied with TEM. As can be seen from these figures, the external and internal structures of black and milky-white paramorphoses are different. The (0001) surface of the black paramorphose is covered with the rectangular growth plates, whereas the (0001) surface of the milky-white paramorphose is covered with the negative rectangular and quadratic etch pyramids. These growth and etch figures are strictly oriented along $[10\bar{1}0]$. High-angle annular dark-field (HAADF) images (see Fig. 6, *c*, *d* and Fig. 7, *c*, *d*) clearly show the polysynthetic twinning of the black paramorphose and the recrystallization of the milky-white paramorphose.

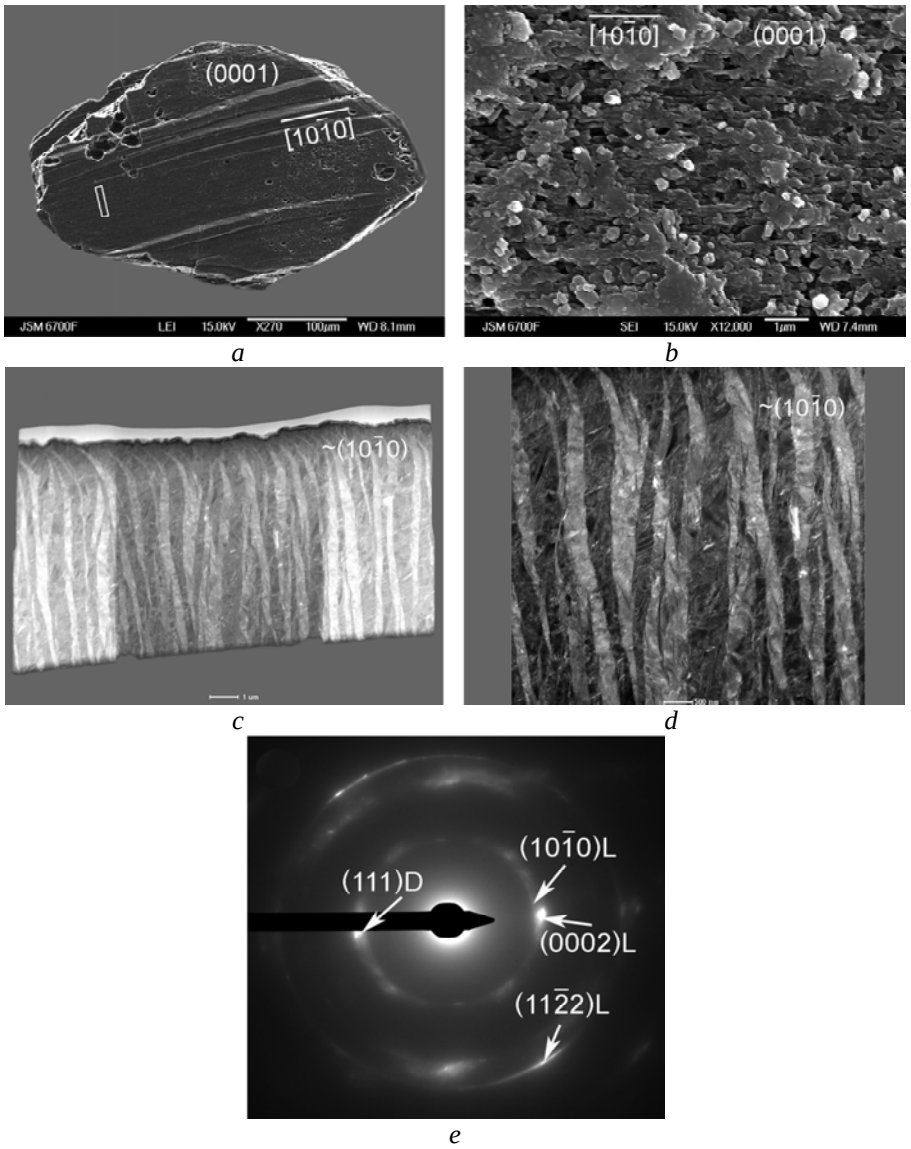

a *b* *c* *d* *e*

Fig. 6. SEM (*a*, *b*) and TEM (*c*–*e*) images of natural impact apographitic diamond: *a* – morphology of a black opaque paramorphose; the location, where the oriented foil 3509 was cut, is indicated by white rectangle; *b* – rectangular growth plates on its (0001) surface; *c* – HAADF image of foil 3509. The darker part of the foil in the center is caused by an additional thinning; *d* – internal structure of the paramorphose, HAADF image with diffraction contrast of twinning, foil 3509; *e* – selected area electron diffraction (SAED) pattern of foil 3509, the scattering intensities are attributed to lonsdaleite (L – lonsdaleite, D – diamond).

Electron diffraction patterns of the foils studied show that the paramorphoses consist of crystallites of lonsdaleite, diamond, and minor graphite. The selected area diffraction patterns represent a larger volume of the foil (approximately 5 μm in diameter). Figure 6, *e* is an electron diffraction pattern of the carbon phases (with lonsdaleite predominating) of apographitic black impact diamond. Most frequently the observed *d*-spacing d_{hkl} is attributed to lonsdaleite (see the table). Figure 7, *e* is an electron diffraction pattern of the carbon phases (with diamond predominating) of apographitic milky-white impact diamond. Most frequently the observed *d*-spacing d_{hkl} is attributed to diamond (table).

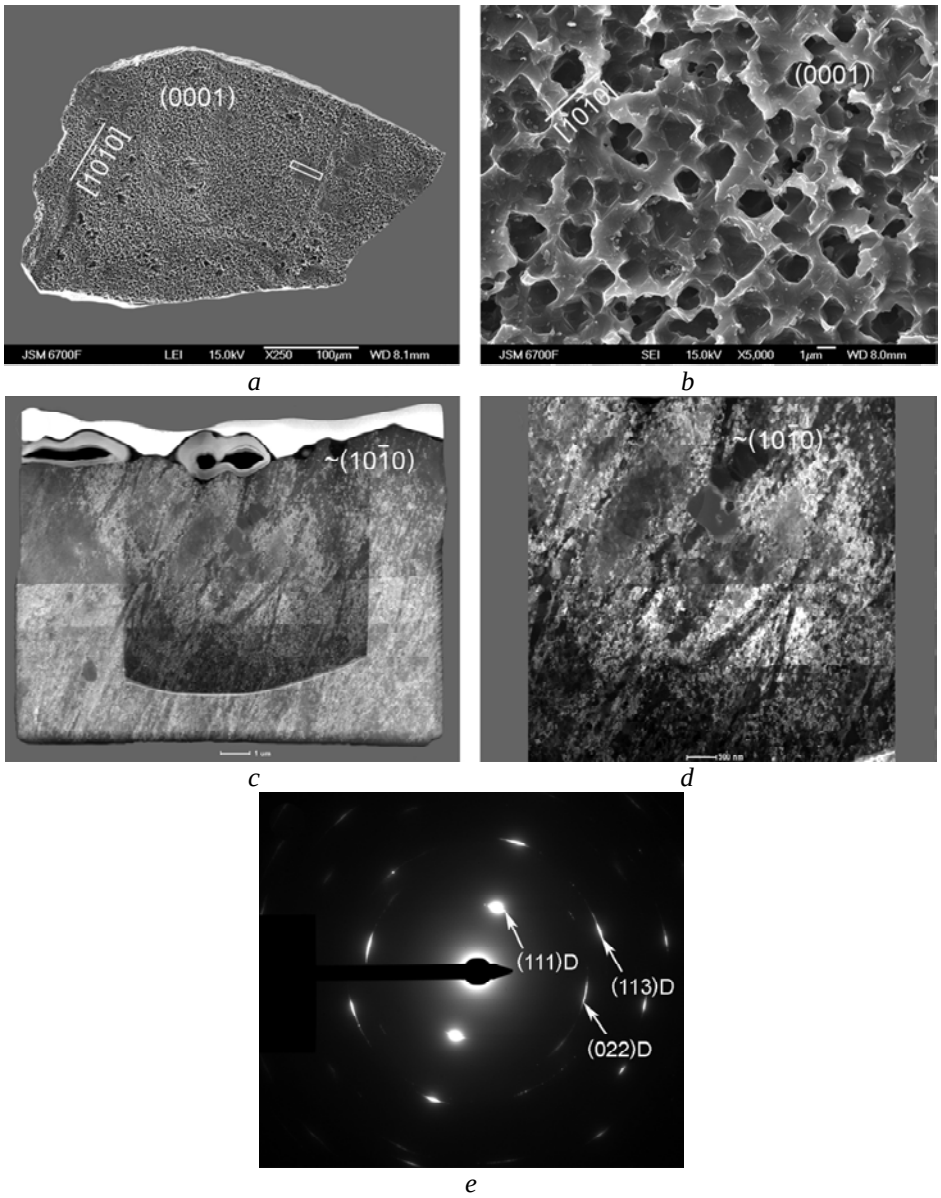

a *b*

c *d*

e

Fig. 7. SEM (*a*, *b*) and TEM (*c*–*e*) images of natural impact apographitic diamond: *a* – morphology of a milky-white opaque paramorphose; the location, where the oriented foil 3510 was cut, is indicated by a white rectangle; *b* – rectangular and quadratic pyramidal etch pits on its (0001) surface; *c* – HAADF image of foil 3510; *d* – internal structure of the paramorphose, HAADF image of recrystallization, foil 3510; *e* – SAED pattern of foil 3510, the scattering intensities are attributed to diamond (D – diamond) only.

TKD analysis: Orientation and Phase relationships at the nm scale

The foil 3510 from the milky-white paramorphose gave a very good TKD map (Fig. 8). The obtained data showed that the sample 3510 is > 95 % diamond, it represents a strongly deformed grain with distinct shear bands. That is, the TKD method confirms it is all diamond, partly recrystallized with some interesting features that are known from extreme deformation in metals.

Interplanar spacings (*d* in Å) for black and milky-white impact diamonds (foils)

Black impact diamond, foil 3509, *d*		Milky-white impact diamond, foil 3510, *d*	Graphite*		Lonsdaleite*		Diamond*	
			d	*hkil*	*d*	*hkil*	*d*	*hkl*
–	2.1502	–	2.1338	$10\bar{1}0$	2.1842	$10\bar{1}0$		
2.0495	2.0507	2.0430	2.0335	$10\bar{1}1$	2.0593	0002	2.0592	111
1.9231	1.9350	–	1.8006	$10\bar{1}2$	1.9296	$10\bar{1}1$		
1.2418	–	1.2525			1.2610	$11\bar{2}0$	1.2610	022
1.2372	1.2390	–	1.2320	$11\bar{2}0$				
1.1457	–	–	1.1565	$11\bar{2}2$	1.1623	$10\bar{1}3$		
1.0632	1.0649	1.0668					1.0754	113
–	–	0.7834					0.7280	242

*2003 JCPDS – International Centre for Diffraction Data.

The foil 3509 from the black paramorphose was too fine-grained i.e. below 20 nm and/or intergrown for a successful automated quantitative mapping analysis (Fig. 9). Analysis of foil 3509 showed that the sample is crystalline (i.e. not amorphous) as there are detectable Kikutchi patterns throughout the sample. The patterns suggest grain-sizes in the nanoscale (< ~ 20 nm) and the crystalline material is strongly intergrown and deformed. According to the latter characteristics, it was not possible to obtain sufficiently good Kikuchi patterns for constructing a reliable phase and/or orientation map. In other words, the nanoscale intergrowth of graphite, diamond and lonsdaleite prevented quantitative analysis.

DISCUSSION

It was shown ealier that already the (0001) surface micromorphology of the black and yellowish paramorphoses allows one to evaluate their phase composition and to determine the orientation relationship between structures of the phases [9]. For these paramorphoses the following orientation relationships between initial graphite and new phases of lonsdaleite and diamond were determined: (0001) graphite is parallel to $(10\bar{1}0)$ lonsdaleite and to (111) diamond (Fig. 10). That orientation relationship suggests a martensitic formation mechanism of impact apographitic diamond and of the direct transition graphite–lonsdaleite and graphite–diamond during shock loading.

The same orientation relationship for the phases of impact diamonds from meteorites have been established [14–16]. But there are different mechanisms of their formation under shock loading: martensitic and topotactic. So, Garvie et al. (2014) [16] examined nano-sized grains of interstratified graphite and diamond from Gujba, an extraterrestrially shocked meteorite, using HRTEM. This coexistence allows them to derive a topotactic mechanism for the transition, complete with the transition matrix. However, in our case, there was a martensitic transformation. This is evidenced by regular orientations of growth and etch figures on the (0001) surface of the paramorphoses as well as a regular orientation of the new phases with respect to the morphology of the original graphite.

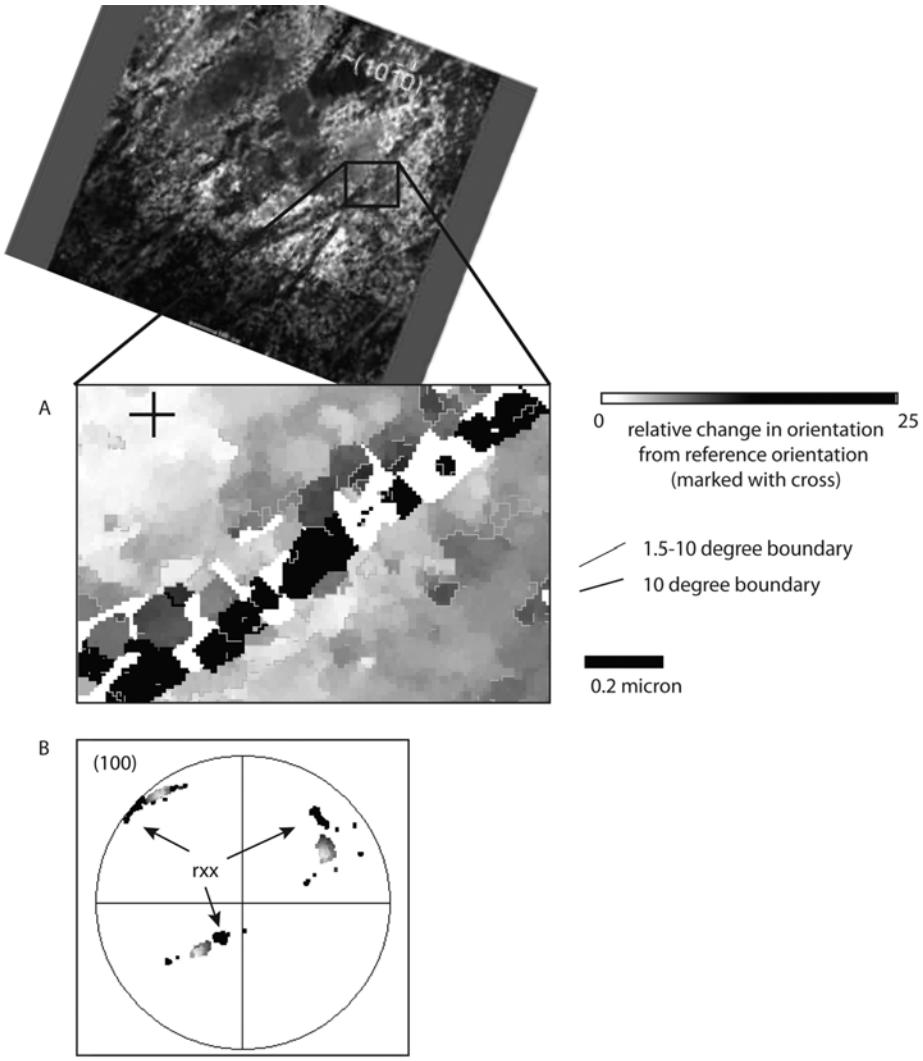

Fig. 8. Orientation characteristics of a deformation shear band present in foil 3510. (A) EBSD orientation map (location of map is shown as black box in overview image) showing in grey scale the change in orientation relative to the reference orientation marked with black cross. Clean white areas are areas where no reliable orientation data could be obtained. 1.5–10 degree boundaries are marked in silver while high-angle boundaries are depicted in black. Note the area of recrystallized grains (dark grey) extending from the right upper corner to the left lower corner. (B) Pole figure showing the orientation of the recrystallized grains relative the deformed "parent" grain. Note the grey scale scheme corresponds to that of the orientation map.

The features of (0001) surface morphology of milky-white paramorphoses document their almost pure diamond phase composition and other relations between the structures of the initial graphite and new phase of diamond (Fig. 11). This is different from what we observe in black and yellowish paramorphoses. Based on the etch figures, the (0001) plane of the initial graphite coincides with the (112) plane of diamond. The $(10\bar{1}0)$ plane of graphite is parallel to (111) plane of diamond. Similar structural orientation relationship of the original graphite and the newly formed phases of lonsdaleite and diamond are described for an experimentally shock-quenched diamond e.g., [17]. This orientation was explained by the serial transformations of graphite → lonsdaleite → diamond. At first, orientation

(0001) graphite perpendicular to (0001) lonsdaleite was implemented. Then the (0001) planes of lonsdaleite transform to the (111) planes of diamond, since the (0001) planes of lonsdaleite are constructed similar to the (111) planes of diamond. So, there is new structural type of natural impact apographitic diamonds: (0001) graphite is parallel to $(10\bar{1}0)$ lonsdaleite and parallel to (112) diamond.

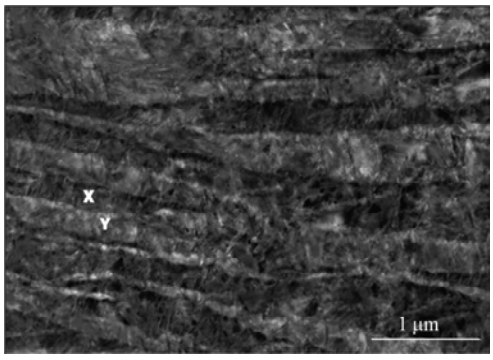

Fig. 9. Orientation contrast image of foil 3509 showing qualitatively different orientations and phases in different grey scale. Note the 0.2–0.4 μm thick bands of different phase/orientation and strong intergrowth within bands at the nanometer scale. Patterns show that elongate areas ("X" versus "Y") do not show a well-defined twinning relationship.

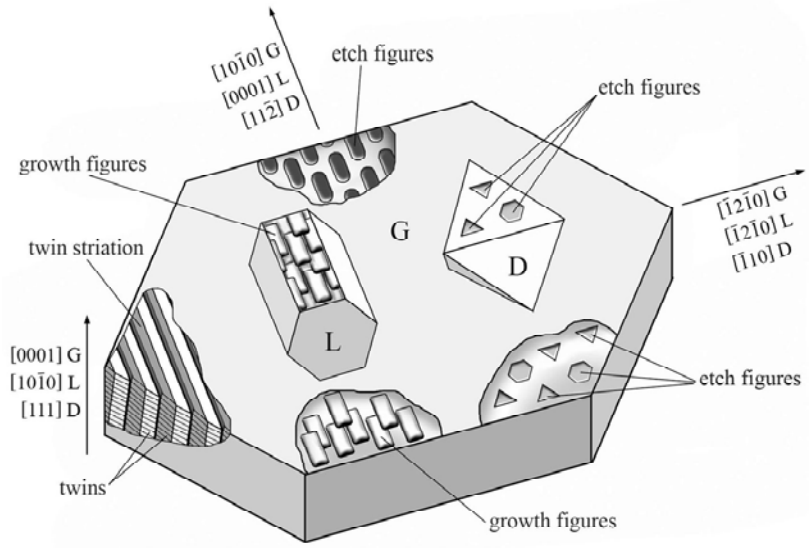

Fig. 10. Orientation relationship of structures of precursor graphite and newly formed lonsdaleite and diamond (G is the graphite crystal, L is a hypothetical lonsdaleite crystal, D is a hypothetical diamond crystal) in black and yellowish paramorphoses. The growth and etch figures on the (0001) surface of the paramorphose. Drawing is slightly modified [9].

Elements of such kind of orientation relationships between graphite–lonsdaleite–diamond were observed for artificial and natural paramorphoses of impact structures by many other researchers, e.g., [5, 18–22]. Sokhor and Futergendler [20] reported that the (111) plane of diamond is parallel to the (0001) plane of lonsdaleite in natural paramorphoses. Also similar structural orientation relationships between graphite, lonsdaleite, and diamond are determined in

artificial paramorphoses, e.g., [6, 21]: (111) diamond is perpendicular to (0001) graphite and (111) diamond parallel to (0001) lonsdaleite.

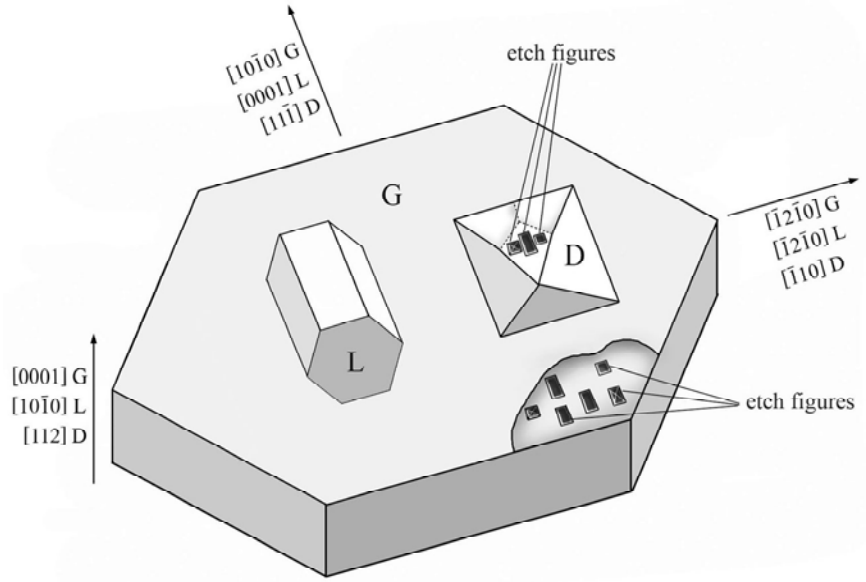

Fig. 11. Orientation relationship of structures of precursor graphite and newly formed lonsdaleite and diamond (G is the graphite crystal, L is a hypothetical lonsdaleite crystal, D is a hypothetical diamond crystal) in the milky-white paramorphoses. The etch figures on the (0001) surface of the paramorphose.

Probably the formation of such milky-white impact diamonds took place at very high temperatures and pressures, when the metastable phase of lonsdaleite transforms into a stable phase of diamond. This was accompanied by growth and high deformation of diamond grains resulting in large highly deformed diamond grains with distinct shear bands characterized by stringers of small, nanometer scale, less deformed diamond grains. This phenomenon of transformation lonsdaleite into diamond at high temperatures under shock loading (32 GPa and above 3200 K) was confirmed by experiments [23].

Our findings provide new insights into epitaxial diamond growth on impact diamonds: time and some growth conditions. Similar epitaxial growth forms (octahedrons, cube-octahedrons and cubes of micro-nanometer sizes) on (0001) planes of natural white paramorphoses have been described earlier [1], but the orientation relationships of the phases involved in such paramorphoses have not been clarified. Recently Masaitis [24] reported the same epitaxial growth on some Popigai impact diamonds. Also Trueb [25] found the same epitaxial growth forms on artificial impact diamonds.

Infrared spectroscopic measurements of natural impact apographitic diamonds indicates that they do not contain impurities of nitrogen (or contain less than the threshold sensitivity of the method, which is less than 20 ppm). However, photoluminescence study indicated the existence of nitrogen complexes (N3 and H3 centers) in milky-white paramorphoses [1]. It can be assumed that just the epitaxial growth forms of the paramorphoses contain impurities of nitrogen. Probably their growth occurred on the diamond matrix by gas phase condensation after the transition of graphite → lonsdaleite → diamond.

CONCLUSIONS

The study of the surface morphology of natural impact apographitic diamonds provides new information on their crystallogenesis:

The (0001) surface morphology of natural impact apographitic diamonds reflects their phase composition and structure type.

There are two structural types of natural impact apographitic diamonds with the following orientation relationships of the phases: the first type (black, colorless and yellowish paramorphoses) – (0001) graphite is parallel to $(10\bar{1}0)$ lonsdaleite and parallel to (111) diamond, the second type (milky-white paramorphoses) – (0001) graphite is parallel to $(10\bar{1}0)$ lonsdaleite and parallel to (112) diamond. The direct transition of graphite → lonsdaleite and graphite → diamond occurs in the first structural type. The successive transition of graphite → lonsdaleite → diamond takes place during the formation of the second structural type.

The structure of milky-white impact apographitic diamonds is totally different from that of the black, colorless, and yellowish impact apographitic diamonds. It appears that the paramorphoses are deformed and partially recrystallized due to high temperature (due to an annealing event) at high shock pressure.

The matrix of milky-white impact apographitic diamonds may consist of polyhedral micro-nanocrystallites of diamond. This is a unique phenomenon of polyhedral growth in a split second due to high shock loads.

The oriented micro-nanopolyhedrons of diamonds – octahedrons – can grow on (0001) surfaces of the paramorphoses of the second structural type. The four fold axis of the polyhedrons and the [001] diamond matrix are parallel.

We thank A. Schreiber (GFZ, Potsdam) for preparing oriented foils for TEM investigations. This is contribution no. 581/988 from the ARC Centre of Excellence for Core to Crust Fluid Systems (www.CCFS.mq.edu.au) and GEMOC(www.GEMOS.mq.edu.au). The authors acknowledge the facilities, and the scientific and technical assistance, of the Australian Microscopy & Microanalysis Research Facility at the Australian Centre for Microscopy and Microanalysis, The University of Sydney.

Вивчено зовнішню і внутрішню морфологію природного імпактного апографітового алмазу – параморфоз. Морфологія поверхонь (0001) параморфоз відображає їх фазовий склад і структурні взаємозв'зки складових фаз. Скульптури росту і травлення з елементами кристалічної симетрії лонсдейліту і алмазу розвинуті на цих поверхнях. Розмір кристалітів лонсдейліту – до 100 нм, а алмазу – до 300 нм. Виявлено два типи структурних співвідношень між графітом, лонсдейлітом і алмазом в параморфозах: перший тип (чорні, чорно-сірі, безбарвні і жовтуваті параморфози) – (0001) графіту паралельна $(10\bar{1}0)$ лонсдейліту і (111) алмазу; другий тип (молочно-білі параморфози) – (0001) графіту паралельна $(10\bar{1}0)$ лонсдейліту і (112) алмазу. Перший тип параморфоз містить лонсдейліт–алмаз–графіт або алмаз–лонсдейліт, другий тип параморфоз – переважно алмаз. Прямий фазовий перехід графіт → лонсдейліт та/або графіт → алмаз відбувся в параморфозах першого типу. Послідовний фазовий перехід графіт → лонсдейліт → алмаз мав місце в параморфозах другого типу. Структура параморфоз цього типу несе характерні ознаки перекристалізації.

***Ключові слова**: природний імпактний апографітовий алмаз, графіт, лонсдейліт, алмаз, морфологія поверхні, структурний тип.*

Изучена внешняя и внутреняя морфология природного импактного апографитового алмаза – параморфоз. Морфология поверхностей (0001) пароморфоз отражает их фазовый состав и структурные взаимоотношения составляющих фаз. Скульп-

туры роста и травления с элементами кристаллической симметрии лонсдейлита и алмаза развиты на этих поверхностях. Размер кристаллитов лонсдейлита – до 100 нм, а алмаза – до 300 нм. Выявлено два типа структурных соотношений между графитом, лонсдейлитом и алмазом в параморфозах: первый тип (черные, черно-серые, бесцветные и желтоватые параморфозы) – (0001) графита параллельна $(10\bar{1}0)$ лонсдейлита и (111) алмаза; второй тип (молочно-белые параморфозы) – (0001) графита параллельна $(10\bar{1}0)$ лонсдейлита и (112) алмаза. Первый тип параморфоз содержит лонсдейлит–алмаз–графит или алмаз–лонсдейлит, второй тип параморфоз – преимущественно алмаз. Прямой фазовый переход графит → лонсдейлит и/или графит → алмаз состоялся в параморфозах первого типа. Последовательный фазовый переход графит → лонсдейлит → алмаз имел место в параморфозах второго типа. Структура параморфоз этого типа несет характерные признаки перекристаллизации.

***Ключевые слова**: природный импактный апографитовый алмаз, графит, лонсдейліт, алмаз, морфология поверхности, структурный тип.*

1. *Вальтер А. А., Еременко Г. К., Квасница В. Н., Полканов Ю. А.* Ударно-метаморфогенные минералы углерода. – К.: Наук. думка, 1992. – 171 с.
2. *Вишневский С. А., Афанасьев В. П., Аргунов К. П., Пальчик Н. А.* Импактные алмазы: их особенности, происхождение и значение (Impact diamonds: their features, origin and significance). – Новосибирск: Изд-во НИЦ ОИГГМ СО РАН, 1997. – 53 с.
3. *Langenhorst F., Shafranovsky G. I., Masaitis V. L., Koivisto M.* Discovery of impact diamonds in a Fennoscandian crater and evidence for their genesis by solid-state transformation // Geology. – 1999. – **27**, N 8. – P. 747–750.
4. *Koeberl C., Masaitis V. L., Shafranovsky G. I. et al.* Diamonds from the Popigai impact structure // Ibid. – 1997. – **25**, N 11. – P. 967–970.
5. *Горогоцкая Л. И., Квасница В. Н., Надеждина Е. Д.* Ориентационные соотношения графит–лонсделеит–алмаз при природных превращениях в ударных волнах // Минерал. журнал. – 1989. – **11**, № 1. – С. 26–33.
6. *Курдюмов А. В., Пилянкевич А. П.* Фазовые превращения в углероде и нитриде бора. – К.: Наук. думка, 1979. – 188 с.
7. *Godinho J. R., Piazolo S., Evans L. Z.* Effect of surface orientation on dissolution rates and topography of CaF_2 // Geochim. Cosmochim. Ac. – 2012. – **86**. – P. 392–403.
8. *Godinho J., Piazolo S., Balic-Zunic T.* Importance of surface structure on dissolution of fluorite: implications for surface dynamics and dissolution rates // Ibid. – 2014. – **126**. – P. 398–410.
9. *Kvasnytsya V., Wirth R.* Micromorphology and internal structure of apographitic impact diamonds: SEM and TEM study // Diam. Relat. Mater. – 2013. – **32**. – P. 7–16.
10. *Wirth R.* Focused ion beam (FIB): A novel technology for advanced application of micro- and nanoanalysis in geoscience and applied mineralogy // Eur. J. Mineral. – 2004. – **16**. – P. 863–876.
11. *Wirth R.* Focused ion beam (FIB) combined with SEM and TEM: advanced analytical tools for studies of chemical composition, microstructure and crystal structure in geomaterials on a nanometer scale // Chemical Geology. – 2009. – **261**. – P. 217–229.
12. *Trimby P. W.* Orientation mapping of nanostructured materials using transmission Kikuchi diffraction in the scanning electron microscope // Ultramicroscopy. – 2012. – **120**. – P. 16–24.
13. *Wyckoff R. W. G.* Crystal Structures. – New York: John Wiley and Sons, 1963. – Vol. 1. – P. 7–83.
14. *Valter A. A., Oleinik G. S., Fisenko A. V., Semenova L. F.* Structural and morphological evidence of the impact-induced development of diamond after graphite in the Novo-Urei meteorite // Geochemistry Int. – 2003. – **41**. – P. 939–946.
15. *Nakamuta Y., Toh S.* Transformation of graphite to lonsdaleite and diamond in the Goalpara ureilite directly observed by TEM // Am. Mineral. – 2013. – 98. – P. 574–581.
16. *Garvie L. A. J., Németh P., Buseck P. R.* Transformation of graphite to diamond via a topotactic mechanism // Ibid. – 2014. – **99**. – P. 531–538.
17. *Wheeler E. J., Lewis D.* The structure of a shock-quenched diamond // Mater. Research Bulletin. – 1975. – **10**, N 7. – P. 687–694.
18. *Bundy F. P., Kasper J. S.* Hexagonal diamond – a new form of carbon // J. Chem. Phys. – 1967. – **46**, N 9. – P. 3437–3446.

19. *Lonsdale K.* Formation of lonsdaleite from single-crystal graphite // Am. Mineral. – 1971. – **56**. – P. 333–336.
20. *Сохор М. И., Футергендлер С. И.* Рентгенографическое исследование образований кубический алмаз–лонсдейлит // Кристаллография . – 1974. – **19**, вып. 4. – С. 759–762.
21. *Курдюмов А. В., Малоголовец В. Г., Новиков Н. В. и др.* Полиморфные модификации углерода и нитрида бора. – М.: Металлургия, 1994. – 318 с.
22. *Oleinik G. S., Valter A. A., Erjomenko G. K.* The structure of high lonsdaleite diamond grains from the impactites of the Belilovka (Zapadnaja) astrobleme (Ukraine) // 34th Lunar and Planetary Sci. Conf. LPI, Houston, Texas, USA, 17–21 March, 2003. – Abstr. No. 1561.
23. *Kurdyumov A. V., Britun V. F., Yarosh V. V. et al.* The influence of the shock compression conditions on the graphite transformations into lonsdaleite and diamond // J. Superhard Mater. – 2012. – **34**, N 1. – P. 19–27.
24. *Масайтис В. Л.* Импактные алмазы Попигайской астроблемы: основные свойства и практическое применение // Зап. Рос. минерал. о-ва. – 2013. – **142**, № 2. – С. 1–10.
25. *Trueb L. F.* An electron-microscope study of shock-synthesized diamond // J. Appl. Phys. – 1968. – **39**, N 10. – P. 4707–4716.

Received 21.04.15